Review

Pancreatic Adenocarcinoma: Imaging Modalities and the Role of Artificial Intelligence

Cristian Anghel , Grasu Cristian Mugur * , Denisa Andreea Anghel , Gina Ionela Rusu-Munteanu , Radu Lucian Dumitru , Ioana Gabriela Lupescu

Posted Date: 11 January 2024

doi: 10.20944/preprints202401.0904.v1

Keywords: pancreatic adenocarcinoma; artificial intelligence; pancreas imaging

Review

Pancreatic Adenocarcinoma: Imaging Modalities and the Role of Artificial Intelligence

Cristian Anghel [1,2], Mugur Cristian Grasu [1,2]*, Denisa Andreea Anghel [2], Gina Ionela Rusu Munteanu [2], Radu Lucian Dumitru [1,2] and Ioana Gabriela Lupescu [1,2]

[1] Carol Davila University of Medicine and Pharmacy Bucharest, Romania
[2] Department of Radiology and Medical Imaging, Fundeni Clinical Institute, Bucharest, Romania
* Correspondence: cristian.grasu@umfcd.ro

Abstract: Pancreatic ductal adenocarcinoma (PDAC) is the most common malignant tumor of the pancreas, carrying a poor prognosis, in most cases patients being diagnosed in a nonresectable stage. Image-based artificial intelligence (AI) models implemented in tumor detection, segmentation and classification could improve diagnosis with better treatment options and increased survival. This review included papers published in the last 5 years and describes the current trends in AI algorithms used in PDAC. We analyzed the applications of AI in detection of PDAC, segmentation of the lesion and classification algorithms used in differential diagnosis, prognosis, and histopathological and genomic prediction. The results show lack of multi-institutional collaboration and stresses the need for bigger datasets in order for AI models to be implemented in a clinically relevant manner.

Keywords: pancreatic adenocarcinoma; artificial intelligence; pancreas imaging

1. Introduction

Pancreatic ductal adenocarcinoma (PDAC) is the most common and aggressive type of malignant tumor of the pancreas, with a five-year relative survival rate of 12% [1]. According to the American Cancer Society about 65,050 people will be diagnosed with pancreatic cancer and about 50,550 people will die of pancreatic cancer in the United States in 2023 [2]. It is currently the 4th leading cause of all cancer deaths in both genders, with data suggesting it will become the 2nd most by 2030[3–7]. The most important risk factors for developing PDAC are tobacco use, obesity, personal history of diabetes or chronic pancreatitis, family history of pancreatic cancer or pancreatitis and certain hereditary conditions (such as Peutz-Jeghers syndrome, von Hippel-Lindau syndrome, hereditary breast and ovarian cancer syndrome, multiple endocrine neoplasia type 1 syndrome) [8–10]. PDAC is in most cases diagnosed in advanced stages, with only a minority of patients having a resectable disease. Early-stage diagnosis remains a challenge because most of the patients have nonspecific symptoms or are asymptomatic until the tumor reaches an advanced stage.

Pancreatic lesions can be visualized through ultrasound and magnetic resonance (MRI) images, but the principal modality for assessing pancreatic adenocarcinoma is contrast-enhanced computer topography (CECT) due to its ability to correctly define the extent of tumor infiltration (especially the blood vessels) and the existence of metastases[11]. Based on the imaging features at diagnosis, patients with PDAC are generally classified into resectable, borderline resectable, unresectable and metastatic disease.

Artificial intelligence (AI) is a branch of computer science that is dedicated to developing models used to perform tasks comparable of a human brain. AI has gained a great interest in oncology because it can integrate high amounts of data to produce personalized recommendations based on each patient's clinical and paraclinical characteristics (serum markers, gene expression, imaging features) [12]. Machine learning, as an AI application, focuses on creating statistical algorithms capable of executing tasks without explicit instructions. This enables a system to autonomously learn and improve through experience. [13]. Deep learning (DL) is a subset of machine learning multiple

 doi:10.20944/preprints202401.0904.v1

hidden layers [14]. Neural networks (CNN) are a type of DL algorithm that is inspired by the neural connections of the human brain and provides a framework to analyze complex data without human intervention, being able to choose the most relevant features. CNN is formed by deep layers of filtering operations that can model complex relationships within data sets[15–17]. A diagram of artificial intelligence hierarchy is presented in Figure 1.

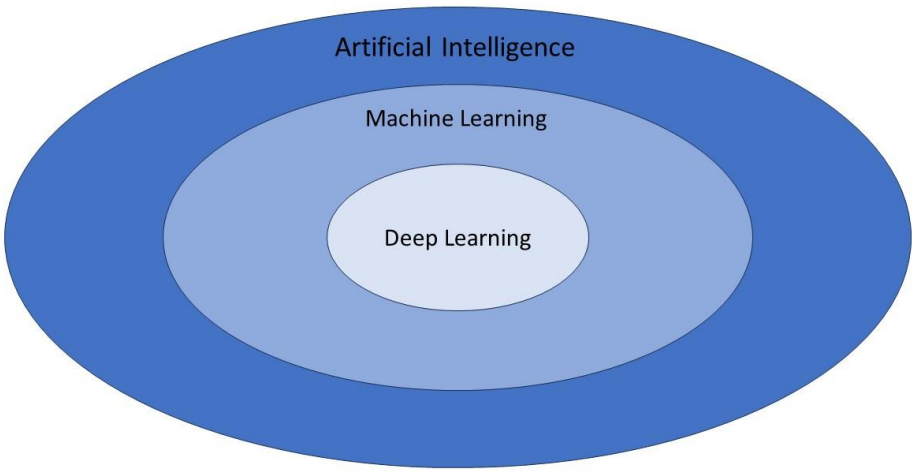

Figure 1. Simplified graphical representation of artificial intelligence hierarchy.

Radiomics aims to extract quantitative information from diagnostic images (CT, MRI, PET, SPECT or ultrasound), including complex patterns that the human eye cannot recognize [18,19]. Combining radiomic data with other patient characteristics (such as biomarkers) has the potential to increase the power of the decision support models. Quantitative image features based on intensity, shape, size, volume and texture can offer information on tumor histopathology and microenvironment [19].Radiomics based machine-learning models have been developed in oncology for diagnosis, prognostic prediction, preoperative staging and assessment of treatment response[20–23]. Radiogenomics represents the correlation between the genomic pattern and the radiomic data. Oncologic patients undergo multiple imaging examinations and in the near future, there will likely be available large data sets comprising images of different histological types, enabling collecting the radiomic features, with the purpose of creating better treatment algorithms and increasing the overall survival.

Our objectives are to review the current imaging protocols for PDAC and to provide an overview of the current AI applications applicable to this pathology. There is an increased interest in AI application in PDAC that is reflected in the number of papers published in the last 5 years. We performed an advanced search on PubMed for articles containing the keywords “pancreatic adenocarcinoma”, “artificial Intelligence” and boolean operators AND. The graph below shows the number of papers published per year with these specific filters (Figure 2).

Preprints (www.preprints.org) | NOT PEER-REVIEWED | Posted: 11 January 2024 doi:10.20944/preprints202401.0904.v1

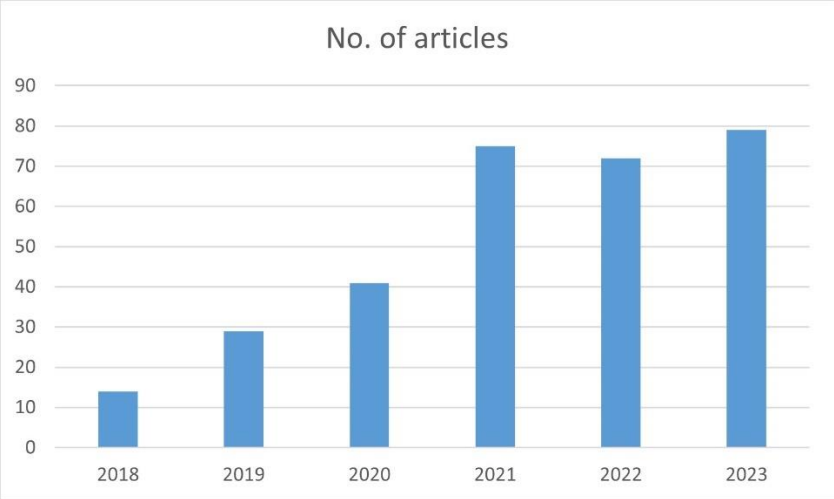

Figure 2. PubMed search for pancreatic adenocarcinoma and artificial intelligence.

2. Imaging modalities

Contrast-enhanced computer tomography (CECT) represents the modality of choice to evaluate PDAC due to its ability to define the vascular involvement of the major blood vessels and to detect the presence of metastases (mainly in the liver, lung and peritoneum). The National Comprehensive Cancer Network (NCCN) guideline recommends the use of CECT as the preferred modality for evaluation at presentation and 4 weeks before surgery and following neoadjuvant treatment for staging and assessment of resectability status[24]. The typical pancreatic CECT protocol is composed of dual-phase acquisition after intravenous contrast medium administration with a pancreatic phase around 35-40 seconds after contrast agent injection and a portal venous phase after a 65 to 70 seconds delay [25]. The advantage of the pancreatic phase consists of better contrast between the increased enhancement of the pancreatic normal parenchyma and the hypoattenuating adenocarcinoma. The portal venous phase allows an easier detection of the hepatic metastases and venous thrombus. One way to improve the enhancement of pancreatic parenchyma and adjacent blood vessels is to use a saline flush in addition to power injection[26]. Resectability criteria are shown in Table 1 [27]. An example of PDAC diagnosed at CECT is shown in Figure 3[24].

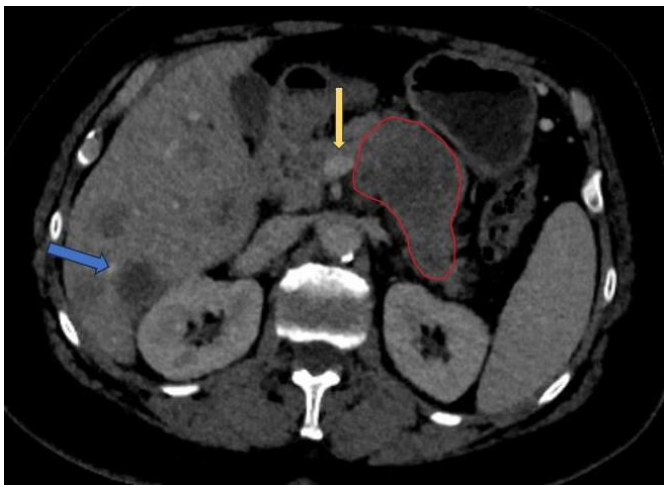

Figure 2. Portal venous phase CT: pancreatic adenocarcinoma involving the corporeal region (red circle) with less than 180° contact with superior mesentery vein (yellow arrow). Multiple liver metastases noted (blue arrow).

MRI has higher soft tissue contrast resolution, but it is not superior to CT in staging of PDAC [28]. According to some studies, MRI is useful in characterizing smaller and isoattenuating tumors

Preprints (www.preprints.org) | NOT PEER-REVIEWED | Posted: 11 January 2024 doi:10.20944/preprints202401.0904.v1

on CT, as well as distinguishing focal fatty infiltration from a tumor [29,30]. The MRI protocol recommended by the NCCN for evaluation of PDAC consists of: T2-weighted imaging (WI) single shot fast spin-echo (SSFSE) in coronal and / or axial; T1WI in-phase and out-phase gradient echo (GRE) in axial plane; T2WI fat-suppressed fast spin-echo (FSE) in axial plane; diffusion weighted imaging (DWI) in axial plane; pre and dynamic post intravenous contrast administration 3D T1WI fat-suppressed GRE in the pancreatic, portal venous and equilibrium phases, in axial plane; and T2WI cholangiopancreatography (MRCP) in coronal plane [24,31]. An example of PDAC diagnosed at MRI is shown in Figure 3. A study by Fang-Ming Chen et al. that compared CT and MRI in the presurgical evaluation of pancreatic cancer on 38 patients showed that the evaluation of vessel involvement, nodal status and resectability had no statistically significant differences between CT and MRI [32].

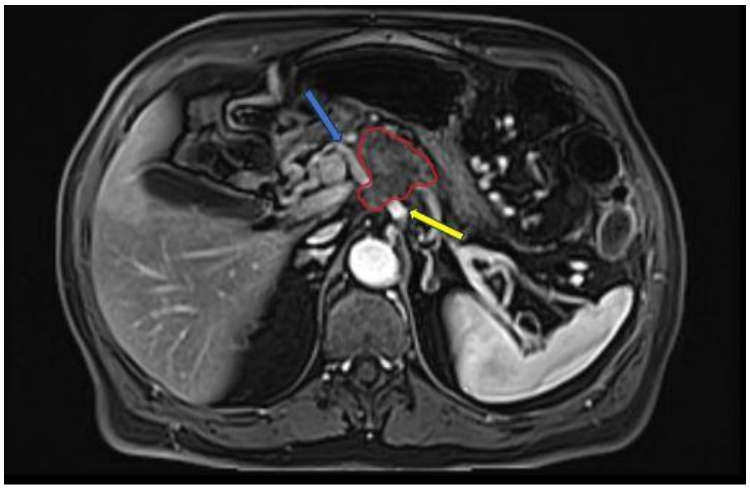

Figure 3. Late-arterial phase 3D T1WI fat-suppressed GRE: pancreatic adenocarcinoma involving the head region (red circle) with less than 180° contact with celiac trunk (yellow arrow) and more than 180° contact with common hepatic artery (blue arrow).

Abdominal ultrasound is a non-invasive diagnostic technique that may be used to diagnose pancreatic lesions. However, it is an operator-dependent modality that in most of the cases does not allow an optimal view and characterization of the entire pancreas because of the gas interposition artefacts. The sensitivity of US in detecting pancreatic adenocarcinoma varies from around 50% to 90% [33,34].

Table 1. Resecability criteria for PDAC.

Resectable	Borderline	Locally Advanced
	Head/uncinate process:	**Head/uncinate process:**
Arterial No contact	Tumor contact with common hepatic artery without extension to celiac artery (CA) or hepatic artery bifurcation. Tumor contact with SMA ≤180°. Tumor contact with variant arterial anatomy.	>180° SMA or CA
	Body/tail:	**Body/tail:**

Preprints (www.preprints.org) | NOT PEER-REVIEWED | Posted: 11 January 2024 doi:10.20944/preprints202401.0904.v1

	Tumor contact with the CA ≤180°	>180° SMA or CA or ≤180° CA and aortic involvement
Venous ≤180° without contour irregularity	>180° or with contour irregularity/thrombosis resection & reconstruction possible. Tumor contact with IVC	Unreconstructible SMV/PV due to tumor involvement or occlusion (can be due to tumor or bland thrombus)

3. AI applications in PDAC

Artificial Intelligence can be used in the detection, segmentation and classification of pancreatic adenocarcinoma.

3.1. Detection

PDAC carries a poor prognosis because of the delayed diagnosis and the lack of screening modalities and protocols in the general population. Studies indicate that detection of PDAC in the high-risk individuals lead to a median overall survival of 9,8 years (compared to 1,5 years for those diagnosed outside of surveillance)[35]. This can be corelated to the fact that early detected tumors are smaller in size and do not infiltrate the surrounding vessels. Identifying small and iso-attenuating tumors can be sometimes difficult, especially in asymptomatic patients, and can lead to delayed recognition[36], [37]. There is a great interest in developing an AI model that could identify PDAC on prediagnostic CTs before the clinical diagnosis. AI algorithms show promise in detecting subtle changes in pancreas and small pancreatic tumors, that can be missed by human observers.

Cao et al. proposes a deep learning model for pancreatic cancer detection with artificial intelligence (PANDA) that can detect and classify pancreatic lesions using non-contrast CT images[38]. The model was trained on a set of non-contrast CT scans of 3208 patients from a single center and achieved an area under the receiver operating curve (AUC) of 0.986-0.996 for lesion detection in a multicenter validation involving 6239 patients across 10 centers.

Korfiatis et al. conducted a case-control study to develop an automated 3-dimensional (3D) Convolutional Neural Network (CNN) for detection PDAC on diagnostic computer tomography scans. One of their objectives was to evaluate the model ability to detect visually occult preinvasive cancer on prediagnostic CTs[39]. The 3D-CNN was trained on data set of 696 portal phase diagnostic CTs with PDAC and 1080 control images with non-neoplastic pancreas and even though was exclusively trained on CTs images with larger tumors, the model managed to detect occult PDAC on prediagnostic CTs (incidentally acquired 3-36 months before clinical diagnosis of PDAC) with AUC curve 0.91, sensitivity 0.75 and specificity 0.90 at a median 475 days before clinical diagnosis.

Chu et al. developed a deep-learning algorithm to classify CT cases from patients with PDAC vs control subjects[40]. Preliminary results from 156 PDAC and 300 normal cases showed 94,1% sensitivity and 98,5% specificity for detection of PDAC. The deep network performed well on larger tumors and often missed small tumors, but this problem could be overcome by adding more small tumors in the training data set and modify the model structure to focus on finding smaller lesions[40].

Another study determined the utility of radiomics features in differentiating CT cases of PDAC from normal pancreas[41]. In this study were included 190 patients with PDAC and 190 healthy potential renal donors, with forty radiomic features selected for analysis. The dataset was divided into 226 training cases (125 normal control cases and 130 PDAC cases) and 125 validation cases (65 normal control cases and 60 PDAC cases). The accuracy of the random forest binary classification was 99.2% and AUC was 99.9%. However, the mean tumor size in this dataset was 4.1 cm, which should not be a problem for the average radiologist to detect. The results need to be validated on datasets containing much smaller tumors.

Preprints (www.preprints.org) | NOT PEER-REVIEWED | Posted: 11 January 2024 doi:10.20944/preprints202401.0904.v1

Chu et al. have also published a paper comparing the diagnostic performance of commercially available vs. in-house radiomics software in classification of CT images from patients with PDAC vs. healthy controls[42]. When 40 features were used in the random forest classification, in-house software achieved superior sensitivity (100%) and accuracy (99,2%) compared to the commercially available research prototype (sensitivity 95% and accuracy 96,8%). However, when the number of features was reduced to five, diagnostic performance of the in-house software decreases to sensitivity (95%) and accuracy (93,6%), while the diagnostic performance of the commercially available prototype was unchanged. The study population was selected based on a previously published study [41]. Future studies are needed to determine if other commercially available radiomics software will achieve similar results.

Man et al. constructed a CNN model using a dataset of 3494 CT images from 222 patients confirmed with PDAC and 3751 images from 190 patients with normal pancreas with the aim to distinguish pancreatic cancer from benign tissue[43]. The plain phase had the same sensitivity (91.58%) as arterial and venous phase, with an accuracy of 95.47% and specificity of 98.27%. Given the lower radiation dose and easier access to non-contrast CT, their model is suitable for PDAC screening.

Alves et al. developed a deep learning model used for PDAC detection, focusing on small lesions[44]. The study included CECT images from 119 pathology proven PDAC patients and 123 patients without PDAC that were used to train a nnUnet for automatic lesions detection and segmentation. The proposed model achieved a maximum AUC of 0.914 in the whole external test and 0.876 in the subgroup of tumors < 2 cm.

Mukherjee et al. developed a radiomics-based machine-learning (ML) model to detect PDAC at the prediagnostic stage[45]. They included prediagnostic CTs (median interval between CT and PDAC diagnosis: 398 days) of 155 patients and an age-matched cohort of 265 patients with normal pancreas, with 34 radiomics features selected. An internal set of 176 patients and 80 publicity available control cases were used for testing. A machine learning classifier, support vector machine (SVM) had a sensitivity of 95.5% and AUC of 0.98.

Wang et al. addressed the issues of consistency and reproducibility of feature extraction (radiomics) and subsequent modeling by investigating the robustness of radiomics features against multiple uncertainty sources such as bin width resampling, image transformation, image noise and segmentation growth/shrinkage[46]. They collected venous-phase CECT images from 181 control subjects and 85 PDAC case subjects and extracted 924 radiomics features using PyRadiomics. The training set was formed from 189 cases (60 cancer and 129 control) and the remaining 77 cases (25 cancer and 52 control) formed the testing set. They trained a Random Forest model using 8 nonredundant radiomics features to distinguish the cancer patients from healthy individuals, which achieved a mean AUC of 0.99 ± 0.01 on the training dataset by cross-validation and an AUC of 0.910 on the independent data set. However, the sample size was limited compared to other published studies[47,48].

Viviers et al. proposed a method based on a U-Net-Like Deep CNN that exploits the external secondary features such as the pancreatic duct, common bile duct and the pancreas, along with a processed CECT scan[49]. The study included a dataset of 99 cases of PDAC located in the pancreatic head and 97 control cases without pancreatic tumor. The model achieved a performance for classification and localization of 99% sensitivity and 99% specificity. However, the CNN model cannot discover the causal relationship between these secondary features and the presence of the tumor, with future work needed to enable a CNN to fully integrate all the information.

Table 2. AI detection models.

Author	Year	Modality	Approach	Sensitivity
Cao et al.[38]	2023	Non-contrast CT	Deep learning	92.9%
Korifatis et al.[39]	2023	CECT	3D-CNN	75%
Alves et al.[44]	2022	CECT	CNN	N.A.
Wang et al.[46]	2022	CECT	Radiomics	84%

Preprints (www.preprints.org) | NOT PEER-REVIEWED | Posted: 11 January 2024 doi:10.20944/preprints202401.0904.v1

Mukherjee et al.[45]	2022	CECT	Radiomics-ML	95.5%
Viviers et al.[49]	2022	CECT	U-Net-Like Deep CNN	99%
Man et al.[43]	2020	Non-contrast CT	CNN	91.58%
Chu et al.[40]	2019	CECT	Deep learning	94,1%
Chu et al.[41]	2019	CECT	Radiomics	100%

3.2. Segmentation

Most of the AI radiology models are supervised and need large amounts of images for training[50]. Image preparation including lesion and organ segmentation is done in most instances manually or in a semi-automated manner by the radiologist. This process needs huge amount of work and given the fact that for AI models to be validated large datasets are needed for training and testing, a great interest in automatic segmentation of the pancreas and pancreatic lesions is seen in the last years. An example of semi-automated tumor segmentation using 3D Slicer software (https://www.slicer.org/) is shown in Figure 4.

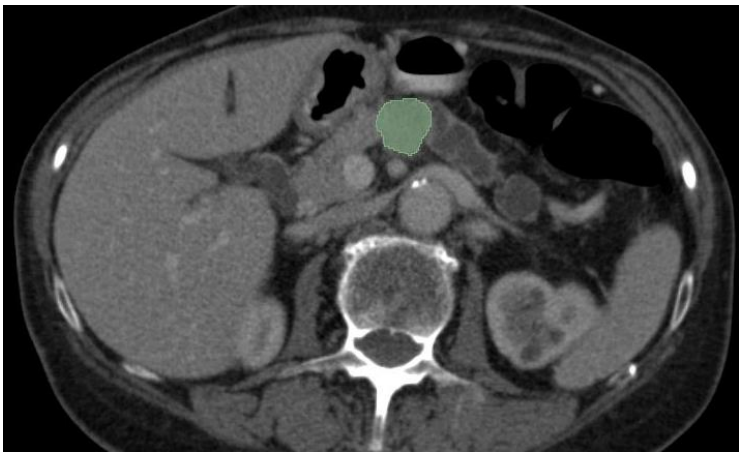

Figure 4. CECT portal venous-phase showing semi-automated corporeal pancreatic tumor segmentation (depicted in green) using "growing-seeds" method.

Automated segmentation of PDAC in CT scans represents a challenge given (1) the variability in size, shape and location of the tumor in the pancreas, (2) small size of the pancreas and the tumor by comparison with the entire abdomen and (3) poor contrast of the pancreas with the surrounding structures[51–53]. AI segmentation algorithms include multiorgan atlas based, landmark based, shape model based, and neural network based[54]. The Dice similarity coefficient (DSC) is used to evaluate the overlap between a predicted segmentation mask and the ground truth segmentation (done manually by the radiologist), with a score that ranges from 0 (no spatial overlap between two sets of binary segmentation results) to 1 (complete overlap).

Ni et al. investigated the reliability of radiomic features extracted from CECT by AX-Unet, a pancreas segmentation model that integrates the strengths of deepLabV series[55], Unet and Xception networks[56], to analyze the recurrence of PDAC after radical surgery[57]. The model was trained on a set of 205 PDAC patients and evaluated on an independent testing set of 64 patients with clear prognoses. The Dice score for their dataset reached 85,9%, showing great effectiveness for PDAC image segmentation.

Tureckova et al. proposed the extension of CNN by including deep supervision and attention gates[58]. The model analyzed a dataset of 421 portal-venous phase CT imaging and segmentation masks for pancreas and tumor captured at memorial Sloan Kattering Cancer Center. 282 of these images are part of the training set release publicity for the 2018 MICCAI Medical Decathlon Challenge[59]. They performed five-fold cross-validation during training with 26 images used for validation and 105 images for training. The dice scores of their VNet-AG-DSV were 81.22% and

Preprints (www.preprints.org) | NOT PEER-REVIEWED | Posted: 11 January 2024 doi:10.20944/preprints202401.0904.v1

52.99% for pancreas and tumor label, respectively. In comparison, Isensee et al. achieved in the MICCAI Medical Decathlon Challenge a dice score for the pancreas and the pancreas-tumor segmentation of 79.30% and 52.12% using a nnU-Net model[60].

The algorithms studied for segmenting PDAC are optimized for only one type of input (one phase of CT acquisition) and therefore the models cannot be implemented in a multi-phase instance. To address this problem, Shen et al. proposed a multi-phase segmentation model, Hyper-Pairing Network (HPN) for better performance for detecting pancreatic tumors[61]. They constructed a dual-path network for handling multi-phase data and applied skip connections across different paths of the network (referred to as hyper-connections) to enable information exchange between different phases. They also applied an additional pairing loss that encourages the commonality between the two sets of high-level semantic representations to reduce view divergence. The model was trained and tested on arterial and venous phase CT images from 239 patients with pathologically proved PDAC. Compared to single-phase algorithms, multi-phase algorithms had a superior DSC (57.10% ± 24.76% for 3D-UNet-multi-phase-HPN and 63.94 ± 22.74 % for 3D-ResDSN-multi-HPN).

Mahmoudi et al. used a 3D-CNN architecture localized the pancreas region from the whole CT volume using 3D Local Binary Pattern (LBP) map of the original image[62]. The pancreatic tumor was subsequently segmented using 2D attenuation U-Net and Texture Attention U-Net (TAU-Net) that was introduced by fusion of dense Scale-Invariant Feature Transform (SIFT) and LBP descriptors intro the attention U-Net. An ensemble model was used to cumulate the advantages of both networks using a 3D-CNN. The Dice global score for the proposed hybrid model auto-localization was 60,6%.

Most of the proposed algorithms for PDAC segmentations have been trained on large tumors, but there is little research focused on early signs of PDAC (such as dilated pancreatic duct). Shen et al. addressed this problem and trained a fully convolutional networks (FCN) to generate an ROI covering the pancreas and used a 3D U-Net-like FCN for coarse pancreas segmentation[63]. The average Dice score and sensitivity was 49,9% and 51,9%, respectively. Their work shows the potential of using AI models for dilated pancreatic duct segmentation.

Table 3. AI segmentation models for PDAC.

Author	Year	Modality	AI Method	DICE score
Ni et al.[57]	2023	CECT	AX-Unet	85,9%
Mahmoudi et al.[62]	2022	CECT	Hybrid 3D-CNN model	60,6%
Tureckova et al.[58]	2020	CECT	VNet-AG-DSV	52,99%
Zhou et al.[61]	2019	CECT	3D-ResDSN-multi-HPN	63.94%
Isensee et al.[60]	2018	CECT	nnU-Net	52,12%

3.2. Classification

3.2.1. Differential diagnosis

Focal-type autoimmune pancreatitis (fAIP) represents a segmental involvement of the pancreatic parenchyma and can mimic PDAC, making the differential diagnosis very difficult. Most of the patients with fAIP will undergo surgical resection for a clear histopathological diagnosis. However, with the development of new AI models, there is hope that a clear discrimination between these entities will be achieved, eliminating the need for patients to undergo future surgical resection. Lu et al. developed a CT-based radiomics nomogram combining subjective CT findings and radiomic features for the preoperative differentiation of fAIP from PDAC[64]. The study included CT images from 96 patients (32 with AIP and 64 with PDAC) with 158 features extracted from each image. 7 features were selected by the LASSO algorithm and a multiparametric radiomics signature was established. They constructed a combined model of radiomics nomogram using multivariate logistic analysis of five characteristics (capsule-like rim, pancreatic atrophy, biliary wall thickening, vascular invasion, and Rad-Score). The nomogram model had a good sensitivity and specificity with AUCs of

 doi:10.20944/preprints202401.0904.v1

0.87 and 0.83 in the training and test cohorts. The study had some limitations, one of them being the low number of fAIP cases acquired over a period of 11 years (2011 to 2021), which are not enough to validate the proposed radiomics model.

Another study conducted by Park et al. on differentiating autoimmune pancreatitis (AIP) from PDAC with radiomics features that included CECT images from 89 patients with AIP and 93 patients with PDAC[65]. Using the CT radiomics features in the test set, AIP could be distinguished from PDAC with a sensitivity of 89.7% (95% CI: 78.6-100%), a specificity of 100% (95% CI: 93-100%), an accuracy of 95.2% (95% CI: 89.8-100%) and an AUC of 0.975 (95% CI: 0.936-1.0). Limitations of the study were the small sample size that included both focal and diffuse forms of AIP and the period of time in which the images were acquired for the patients with AIP (2004 to 2018).

Anai et al, constructed a support vector machine (SVM) classifier using CT textured analysis for differentiating fAIP and PDAC and to assess the radiologist's (4) diagnostic performance with or without SVM[66]. The study included CECT images from 20 patients with fAIP and 30 patients with PDAC from which 62 texture-based features were extracted. The SVM classifier had a high performance in differentiating fAIP and PDAC, with an AUC of 0.920. The SVM classifier increased the AUC for all 4 readers, but the reader with less experience befitted the most from the SVM outputs. However, given the small number of patients included in the study, there is need for larger study population to confirm the results.

Mass-forming chronic pancreatitis (MFCP) is another benign condition that can easily mimic PDAC lesions. A study addressed the problem of discriminating between PDAC and mass-forming chronic pancreatitis lesions (MFCP)[67]. This retrospective study included 119 patients from two independent institutions that had performed preoperative MRI. They extracted four feature sets from T1-weighted imaging (T1WI), T2-weighted imaging (T2WI), arterial phase and portal phase of dynamic contrast-enhanced MRI and radiomics models were constructed. The study shows good results with AUCs for the T1WI, T2WI, arterial and portal phases of 0.893, 0.911, 0.958 and 0.997 in the primary cohort and 0.882, 0.902, 0.920 and 0.962 in the validation cohort. We can see that the best result was obtained on the portal phase of dynamic contrast-enhanced MRI. Some limitations of the study are the small sample size and the fact that the analysis of the area of interest was performed in a two-dimensional manner rather than a three-dimensional analysis of the entire volume of the lesion.

Ren et al. proposed a CT-based radiomics signature for the differential diagnosis between pancreatic adenosquamous carcinoma (PASC) and PDAC[68]. They used CECT images (both late arterial phase and portal venous phase) from 81 patients with PDAC and 31 patients with PASC to extract radiomics features. Seven radiomics features from late arterial phase images and three from portal venous phase images were selected and a radiomics signature was constructed. Using a 10-times leave group our-cross-validation method (LGOCV) the radiomics signature was proved to be robust and reliable with an average AUC of 0.82. However, the limitations of the study were the small number of PASC patients, different scanners used for image acquisition and a selection bias due to retrospective nature of the study.

Shi et al. evaluated the performance of the histogram array and CNN based on diffusion-weighted imaging (DWI) with multiple b-values to distinguish PDAC from solid pseudopapillary neoplasm (SPN) and pancreatic neuroendocrine neoplasm (PNEN)[69]. They included 231 patients (132 PDACs, 45 PNENs and 54 SPNs), which were further divided in a training group (n=92), validation group (n=46) and testing group (n=93). The DWI images from 10 b values were converted into a histogram array that was input into the CNN model. The AUCs of CNN for distinguishing PDACs from non-PDACS were 0.896, 0.846 and 0839 in the training, validation and testing groups. One of the limitations of the study was the low number of PNENs and SPNs used for training the CNN models, given the fact that these pancreatic tumors are rare compared to PDAC[70]. The study also did not include other types of pancreatic tumors such as metastases, mucinous tumors or lymphoma.

Zhang et al assessed the diagnostic ability of radiomics combined with multiple machine learning algorithms to differentiate PDAC from pancreatic neuroendocrine tumor (pNET) by building 45 discriminative models by five selection algorithms and nine classification algorithms[71].

Preprints (www.preprints.org) | NOT PEER-REVIEWED | Posted: 11 January 2024 doi:10.20944/preprints202401.0904.v1

The study included CECT images from 238 patients (156 diagnosed with PDAC and 82 diagnosed with pNET). By using the combination of Gradient Boosting Decision Tree (GBDT) as the selection algorithm and Random Forest (RF) as the classification algorithm the model reached the highest AUC: 0.971 in the training set and 0.930 in the validation set. Their study reinforces the idea that multi-algorithm modeling should be considered when predicting subtypes of cancer with machine learning.

Table 3. AI models studied in differential diagnosis of PDAC.

Author	Year	Modality	Scope	Approach	AUC
Lu et al.[64]	2023	CECT	fAPI vs PDAC	Radiomics	0.83
Shi et al.[69]	2023	MRI	PDAC vs PNEN and SPN	CNN	0.839
Zhang et al.[71]	2022	CECT	PDAC vs pNET	Radiomics	0.930
Anai et al.[66]	2022	CECT	fAPI vs PDAC	Radiomics	0.920
Deng et al.[67]	2021	MRI	MFCP vs PDAC	Radiomics	0.962
Ren et al.[68]	2020	CECT	PASC vs PDAC	Radiomics	0.82
Park et al.[65]	2020	CECT	AIP vs PDAC	Radiomics	0.975

3.2.2. Histopathological subtype and genomic features

Histopathological subtype is a crucial factor in PDAC prognosis, with poor differentiated tumors showing higher aggression and shorter survival than well-differentiated PDAC[72,73]. Poor differentiation represents an independent prognostic factor that affects overall survival in patients with PDAC[74]. Knowing the histopathological grade before the surgical intervention might change the treatment options for patients with poor differentiated tumors, however the histopathological grade is often determined after surgery. It still remains a challenge to determine the histopathological grade of the tumor due to marked morphological tumor heterogeneity and the limited amount of tumor tissue samples in cases of tumor biopsy[75–78]. Developing a noninvasive technique to differentiate between the subtypes of PDAC before treatment could help to maximize patient survival and avoid the risks associated with surgical resection.

Qiu et al. constructed a score using support-vector machine (SVM) to predict the histopathological grade (low/high-grade) of PDAC based on preoperative CECT images from 56 patients[79]. They developed four models: all texture features, histogram features, run-length features, and co-occurrence features. With all texture features, their model predicted low-grade/high-grade PDAC with 86% accuracy, 78% sensitivity and 95% specificity. The study enrolled a small number of patients and needs further validation in a prospective multicenter study.

Another retrospective study studied preoperative clinical-radiomics nomograms using features from CECT images to discriminate high-grade and low-grade PDAC and predict overall survival (OS)[80]. A model was constructed to predict histological grade based on radiomics scores from CECT (HGrad) with an AUC of 0.75 (95% CI: 0.64, 0.85) and 0.76 (95%CI: 0.60, 0.91) in test and validation cohorts. However, their model was based on information obtained in part from biopsy, which can be potentially inaccurate given the fact that only a small sample of the tumor is analyzed.

The most frequent genes that are altered in PDAC are KRAS, CDKN2A, TP53 and SMAD4[81]. Unfortunately, these markers can only be obtained from biopsy specimens or resected lesions. Developing AI models to facilitate the prediction of this markers in PDAC could provide a better therapy option for the patient, without the need for tumor resection.

Hinzpeter et al. investigated the correlation between CECT derived radiomics and driver gene mutations in patients with PDAC in a retrospective study that included 47 patients treated surgically for PDAC[82]. They constructed two statistical models to evaluate the predictive ability of CT-derived radiomics features for driver gene mutations. They obtained an acceptable predictive ability for

Preprints (www.preprints.org) | NOT PEER-REVIEWED | Posted: 11 January 2024 doi:10.20944/preprints202401.0904.v1

KRAS and TP52 with an Youden Index of 0.56 and 0.67, and mild to acceptable predictive ability for SMAD4 and CDKN2A with an Youden Index of 0.5. One limitation of the study was that they did not discriminate between different molecular subtypes of PDAC, which may have important prognostic implications.

In a study conducted by Gao et al. were assessed the preoperative prediction of TP53 status based on MRI radiomics extracted from seven different sequences: dynamic contrast enhanced (DCE) T1-weighted imaging (pre-contrast, late arterial phase (ap), portal venous phase, delayed phase), T2-weighted imaging (T2WI), diffusion-weighted imaging (DWI) and apparent diffusion coefficient (ADC)[83]. They used PyRadiomics package to generate 558 two dimensional (2D) and 994 three-dimensional (3D) images features and further constructed models using SVM. The best performance was achieved by the 3D ADC-ap-DWI-T2WI model with 11 selected features, with an accuracy of 91% and AUC of 0.96. Some limitations of the study were the small number of patients (57) and the fact that the images were acquired on 1.5 T MRI scanners or 3.0 T MRI scanners and there is limited data on whether there is a clear effect of field strength on radiomics characteristics.

The high expression of Mucin 4 (MUC4), a highly glycosylated membrane-bound protein, promotes tumor cell metastasis and tumor cell resistance to chemotherapy[84,85]. The overexpression of MUC4 is associated with an unfavorable prognosis in patients diagnosed with PDAC[86]. Deng et al. explored the utility of radiomics based on MRI to predict the status of MUC4 expression in PDAC preoperatively in a retrospective study that included 52 patients[87]. Two feature sets were extracted from arterial and portal phases and after univariate analysis, minimum redundancy maximum relevance and principal component analysis, the features with a cumulative variance of 90% were selected to construct a radiomics model. They also developed a clinical model. The AUC values of the arterial model, portal model and combined model were 0.732, 0.709 and 0.861. The study suggests that combining the arterial phase model, portal phase model and the clinical model together, the predictive value of the status of MUC4 expression would increase. However, the model needs further external validation on larger samples.

Iwatate et al. examined the relationship between p53 mutations, PD-L1 abnormal expression and clinicopathological factors in order to construct prediction models.[88] The retrospective study included 107 patients diagnosed with PDAC with CECT images (early and late-phase images) that were used for features extraction. The AUC for p53 and PD-L1 predictive models were 0.795 and 0.683. The p53-positive and PD-L1 positive groups were associated with poor prognosis (p=0.006, 0.013). Larger prospective studies need to be conducted to support the results of this study.

Prediction of fibroblast activation protein (FAP) expression in patients with PDAC was studied by Meng et al. on a population of 129 patients with pathology confirmed PDAC[89]. They constructed a multiplayer perceptron (MLP) network classifier based on radiomics features from noncontrast MRI (breath-hold single-shot fast-spin echo T2-weighted sequence and unenhanced and non-contrast T1-weighted fat-suppressed sequences). Their predictive model had an AUC of 0.84 for the training set and 0.77 for the validation set. One limitation of the study was that the images were obtained from a single MRI machine, so further validation on images from other machines needs to be conducted.

Table 3. AI models studied in histopathological and genomic features.

Author	Year	Modality	Scope	Approach	Performance
Cen et al.[80]	2023	CECT	Histopathological grade	Radiomics	AUC 0.76
Deng et al.[87]	2022	MRI	MUC4 expression	Radiomics	AUC 0.861
Hinzpeter et al.[82]	2022	CECT	Correlation with driver gene mutations	Radiomics	Youden Index 0.56 (KRAS), 0.67 (TP53), 0.5 (SMAD4 and CDKN2A)

Preprints (www.preprints.org) | NOT PEER-REVIEWED | Posted: 11 January 2024 doi:10.20944/preprints202401.0904.v1

Gao et al.[83]	2021	MRI	TP53 mutation	Radiomics	AUC 0.96
Meng et al.[89]	2021	MRI	FAP expression	Radiomics	AUC 0.77
Iwatate et al.[88]	2020	CECT	P53 and PD-L1 expression	Radiomics	AUC 0.795 and 0.683
Qiu et al.[79]	2019	CECT	Histopathological grade	Radiomics	Accuracy 86%

3.2.3. Prognosis

In recent years, there has been a notable surge in interest regarding the utilization of radiomic features for predicting the prognosis of PDAC. Vezakis et al. evaluated a fully automated pipeline for survival prediction[90]. They trained an nnU-Net (3D-CNN) on an external dataset and generated automated pancreas and tumor segmentations. The radiomics features were extracted from CECT images from a population of 40 PDAC patients. These features were combined with the TNM system staging parameters and the patient's age. A random forest model was trained to perform an overall prediction overt time and random forest classifier for the binary classification of two-year survival. Their results show promise, achieving a mean C-index of 0.731 for survival modeling and a mean accuracy of 0.76 in two-year survival prediction. One limitation of the study was that given the fully automated manner of the model, segmentation inaccuracies may lead to suboptimal radiomics features extraction.

Xu et al. developed an MRI-radiomics nomogram for the prognosis of PDAC that achieved a C-index of 0.780[91]. The limitations of the study were the small population (78 PDAC patients) and absence of external validation.

Qiu et al. constructed a prognostic model based on preoperative MRI radiomics nomogram for patients with PDAC[92]. To minimize the bias cause by confounding factors they used T2-weighted imaging sequence for radiomics analysis. They calculated a radiomics signature (Rad-score) based on the radiomics features that were significantly related to overall survival (OS) and progression-free survival (PFS). By incorporating the Rad-score and the clinical parameters they made a clinical-radiomics nomogram. The clinical-radiomics nomogram had a C-index for OS and PFS in development cohort of 0.814 and 0.767.

In another study conducted by Li et al. a radiomics-clinical nomogram integrating intra- and peritumoral CT radiomics signature and clinical factors was built in order to assess the recurrence risk of PDAC after radical resection[93]. The radiomics-nomogram showed an AUC of 0.764 (95% CI: 0.644-0.859) in the validation test for predicting 1-year recurrence and an AUC of 0.773 (95% CI: 0.654-0.866) in the validation test for predicting 2-year recurrence.

Xie et al. constructed a radiomics nomogram integrating the Rad-score (from CT images) and clinical data that showed better performance of the survival prediction that the clinical model and TNM staging system with a C index of 0.742 (95% CI: 0.697-0.787) for training cohort and 0.726 (95% CI: 0.646-0.806) for validation cohort[94]. The Rad-score was calculated in a manually fashion, which is time consuming and not feasible in clinical setting.

In another study that evaluated the preoperative CT radiomics features in predicting postoperative survival of patients with PDAC the C-index of survival prediction with clinical parameters alone was 0.6785, while the addition of CT radiomics features improved the C-index to 0.7414[95].

Ni et al. investigated the use of radiomic features extracted from CECT by a pancreas segmentation model to analyze the recurrence of PDAC after radical surgery[57]. The AUC for the nomogram predicting whether the patients will have recurrence after surgery was 0.92 (95% CI: 0.78-0.99) and the C index was 0.62 (95% CI: 0.48-0.78).

Another study analyzed the use of radiomics features extracted from portal venous CT for predicting surgical portal-superior mesenteric vein (PV-SMV) invasion in patients with PDAC[96]. The radiomics signature had an AUC of 0.848 (95% CI: 0.724-0.971) in the validation cohort. One limitation of the study was the exclusion of patients that received neoadjuvant therapy before surgery. Their model shows promising results and should be tested on larger data sets, including

 doi:10.20944/preprints202401.0904.v1

patients who received neoadjuvant therapy, because conventional cross-sectional imaging often can't precisely identify the extent of the remaining viable tumor[97,98].

Prediction of lymph node (LN) status before surgical resection could have an important impact in treatment of PDAC. Three papers focused on predicting lymph node involvement[99–101]. Bian et al. constructed a prediction nomogram that incorporated the radiomics signature (features extracted from arterial CT scans) and CT-reported LN status to LN metastasis, that had AUC of 0.75 (95% CI: 0.68-0.82) in the training cohort and 0.81 (95% CI: 0.69-0.94) in the validation cohort[100]. Shi et al. made a radiomics nomogram constructed by radiomics score for T2WI combined with portal venous phase T1TW and MRI-reported LN status that showed an AUC of 0.845 for the training cohort and 0.816 for the validation cohort[99]. Chang et al. constructed a 3D-CNN model that predicted lymph node status with an accuracy of 90% for per-patient analysis and 75% for per-scan analysis[101].

4. Discussion

PDAC carries a poor prognosis and great work is done in the research world to improve every step in the pathway and management of this malignant tumor. An important factor in prognosis of PDAC is tumor size, with smaller tumors being less invasive in the surrounding tissues, making them resectable. However, giving the non-specific symptomatology, most patients are diagnosed at a later stage. Detecting tumors at small dimensions (preferably <2 cm) is crucial for having a resectable tumor. We believe that one of the main focuses of AI applications should be the detection of small pancreatic tumors. Because most of the tumors are large at diagnosis, the AI-models are trained on data sets that contain a small proportion of small tumors, making it hard for the model to achieve good results in detecting small and isoattenuating PDAC. Large datasets that contain an increased number of small tumors should be made publicly in order for researchers to be able to train their models on and have better results in detecting small (even < 1 cm) tumors in high-risk patients. Two studies have focused on detecting PDAC in NECT[38,43], which in the future could represent a screening method in the high-risk population, given the lower dose compared to CECT and the absence of risk given by the administration of intravenous contrast.

One of the biggest inconveniences found in the studies that focused on PDAC was the lack of an automated pancreatic or tumor segmentation models. Segmentation is time-consuming, needs an experienced radiologist and is not feasible in a clinical setting. Developing automated segmentation AI-software should make research less time-consuming and could increase the number of patients in the datasets, improving the results. However, the studies that we found focused on segmentation on CECT images but given the increasing number of MRI machines available in the world, we believe that further studies need to focus on segmentation on different MRI sequences, making the models applicable both on CT and MRI images.

Current research that analyzed the differential diagnosis of PDAC from other types of pancreatic lesions have been conducted in a binary fashion (distinguishing PDAC from another type of pancreatic lesions, for example neuroendocrine tumors), however for a model to be clinically relevant it should be able to distinguish between a more complex number of pathologies (for example autoimmune pancreatitis, chronic pancreatitis, cystic lesions, and other malignancies). We believe that in the future, research should focus on both detection of correct classification among a variety of pancreatic disease.

Knowing the histopathological grade and the expression of different genes before the surgical intervention might change the treatment options for selected patients, however the histopathological analysis is often determined after surgery. The studies we encountered, which concentrated on genomics and histopathological grading, were conducted on a limited number of cases and require additional validation on larger datasets. However, we anticipate that in the future, AI models could predict the expression of various genes involved in PDAC, leading to personalized therapy becoming a common practice in more healthcare centers.

In terms of survival predictions, the majority of the papers we reviewed focused on patients with resectable disease. Nonetheless, it is crucial to emphasize that a large number of PDAC patients are

diagnosed at an unresectable stage. We advocate for further research to explore multiple treatment options, employing models that predict responses to chemo/radiotherapy.

5. Conclusion

Important advances have been made in the research of artificial intelligence models in PDAC, however multi-institutional collaboration is needed and further validation on bigger datasets should be made in order to construct algorithms ready to be implemented in clinical institutions.

Author Contributions: Conceptualization, C.A, D.A.A.; resources, M.C.G, R.L.D, G.I.R.M.; writing—original draft preparation, C.A..; writing—review and editing, M.C.G..; supervision, I.G.L. All authors have read and agreed to the published version of the manuscript.

Funding: This research received no external funding.

Conflicts of Interest: The authors declare no conflict of interest.

References

1. R. L. Siegel, K. D. Miller, N. S. Wagle, and A. Jemal, "Cancer statistics, 2023," *CA Cancer J Clin*, vol. 73, no. 1, pp. 17–48, Jan. 2023, doi: 10.3322/caac.21763.
2. American Cancer Society, "Facts & Figures 2023."
3. B. Boursi *et al.*, "A Clinical Prediction Model to Assess Risk for Pancreatic Cancer Among Patients With New-Onset Diabetes," *Gastroenterology*, vol. 152, no. 4, pp. 840-850.e3, Mar. 2017, doi: 10.1053/j.gastro.2016.11.046.
4. A. P. Klein *et al.*, "An Absolute Risk Model to Identify Individuals at Elevated Risk for Pancreatic Cancer in the General Population," *PLoS One*, vol. 8, no. 9, p. e72311, Sep. 2013, doi: 10.1371/journal.pone.0072311.
5. R. Pannala, A. Basu, G. M. Petersen, and S. T. Chari, "New-onset diabetes: a potential clue to the early diagnosis of pancreatic cancer," *Lancet Oncol*, vol. 10, no. 1, pp. 88–95, Jan. 2009, doi: 10.1016/S1470-2045(08)70337-1.
6. W. Muhammad *et al.*, "Pancreatic Cancer Prediction Through an Artificial Neural Network," *Front Artif Intell*, vol. 2, May 2019, doi: 10.3389/frai.2019.00002.
7. A. Adamska, A. Domenichini, and M. Falasca, "Pancreatic Ductal Adenocarcinoma: Current and Evolving Therapies," *Int J Mol Sci*, vol. 18, no. 7, p. 1338, Jun. 2017, doi: 10.3390/ijms18071338.
8. S. Solomon, S. Das, R. Brand, and D. C. Whitcomb, "Inherited Pancreatic Cancer Syndromes," *The Cancer Journal*, vol. 18, no. 6, pp. 485–491, Nov. 2012, doi: 10.1097/PPO.0b013e318278c4a6.
9. V. Rosato, J. Polesel, C. Bosetti, D. Serraino, E. Negri, and C. La Vecchia, "Population Attributable Risk for Pancreatic Cancer in Northern Italy," *Pancreas*, vol. 44, no. 2, pp. 216–220, Mar. 2015, doi: 10.1097/MPA.0000000000000251.
10. V. Rosato, J. Polesel, C. Bosetti, D. Serraino, E. Negri, and C. La Vecchia, "Population Attributable Risk for Pancreatic Cancer in Northern Italy," *Pancreas*, vol. 44, no. 2, pp. 216–220, Mar. 2015, doi: 10.1097/MPA.0000000000000251.
11. L. Marti-Bonmati *et al.*, "Pancreatic cancer, radiomics and artificial intelligence," *British Journal of Radiology*, vol. 95, no. 1137. British Institute of Radiology, Sep. 01, 2022. doi: 10.1259/bjr.20220072.
12. B. H. Kann, A. Hosny, and H. J. W. L. Aerts, "Artificial intelligence for clinical oncology," *Cancer Cell*, vol. 39, no. 7, pp. 916–927, Jul. 2021, doi: 10.1016/j.ccell.2021.04.002.
13. H. Hayashi *et al.*, "Recent advances in artificial intelligence for pancreatic ductal adenocarcinoma," *World Journal of Gastroenterology*, vol. 27, no. 43. Baishideng Publishing Group Inc, pp. 7480–7496, Nov. 21, 2021. doi: 10.3748/wjg.v27.i43.7480.
14. S. Do, K. D. Song, and J. W. Chung, "Basics of Deep Learning: A Radiologist's Guide to Understanding Published Radiology Articles on Deep Learning," *Korean J Radiol*, vol. 21, no. 1, p. 33, 2020, doi: 10.3348/kjr.2019.0312.
15. V. Couteaux *et al.*, "Kidney cortex segmentation in 2D CT with U-Nets ensemble aggregation," *Diagn Interv Imaging*, vol. 100, no. 4, pp. 211–217, Apr. 2019, doi: 10.1016/j.diii.2019.03.001.
16. P. Roca *et al.*, "Artificial intelligence to predict clinical disability in patients with multiple sclerosis using FLAIR MRI," *Diagn Interv Imaging*, vol. 101, no. 12, pp. 795–802, Dec. 2020, doi: 10.1016/j.diii.2020.05.009.
17. S. Rastegar *et al.*, "Radiomics for classification of bone mineral loss: A machine learning study," *Diagn Interv Imaging*, vol. 101, no. 9, pp. 599–610, Sep. 2020, doi: 10.1016/j.diii.2020.01.008.
18. S. S. F. Yip and H. J. W. L. Aerts, "Applications and limitations of radiomics," *Phys Med Biol*, vol. 61, no. 13, pp. R150–R166, Jul. 2016, doi: 10.1088/0031-9155/61/13/R150.
19. R. J. Gillies, P. E. Kinahan, and H. Hricak, "Radiomics: Images Are More than Pictures, They Are Data," *Radiology*, vol. 278, no. 2, pp. 563–577, Feb. 2016, doi: 10.1148/radiol.2015151169.

20. L. Shi *et al.*, "Radiomics for Response and Outcome Assessment for Non-Small Cell Lung Cancer," *Technol Cancer Res Treat*, vol. 17, p. 153303381878278, Jan. 2018, doi: 10.1177/1533033818782788.
21. X. Zheng *et al.*, "Deep learning radiomics can predict axillary lymph node status in early-stage breast cancer," *Nat Commun*, vol. 11, no. 1, p. 1236, Mar. 2020, doi: 10.1038/s41467-020-15027-z.
22. A. S. Tagliafico, M. Piana, D. Schenone, R. Lai, A. M. Massone, and N. Houssami, "Overview of radiomics in breast cancer diagnosis and prognostication," *The Breast*, vol. 49, pp. 74–80, Feb. 2020, doi: 10.1016/j.breast.2019.10.018.
23. Y. Huang *et al.*, "Development and Validation of a Radiomics Nomogram for Preoperative Prediction of Lymph Node Metastasis in Colorectal Cancer," *Journal of Clinical Oncology*, vol. 34, no. 18, pp. 2157–2164, Jun. 2016, doi: 10.1200/JCO.2015.65.9128.
24. NCCN, "https://www.nccn.org/professionals/physician_gls/pdf/pancreatic.pdf," Accesed on 10.12.2023.
25. R. R. Almeida, G. C. Lo, M. Patino, B. Bizzo, R. Canellas, and D. V. Sahani, "Advances in Pancreatic CT Imaging," *American Journal of Roentgenology*, vol. 211, no. 1, pp. 52–66, Jul. 2018, doi: 10.2214/AJR.17.18665.
26. H. Schoellnast *et al.*, "Improvement of parenchymal and vascular enhancement using saline flush and power injection for multiple-detector-row abdominal CT," *Eur Radiol*, vol. 14, no. 4, pp. 659–664, Apr. 2004, doi: 10.1007/s00330-003-2085-3.
27. Frank Wessels, Otto van Delden, and Robin Smithuis, "Pancreatic Cancer - CT staging 2.0," https://radiologyassistant.nl/abdomen/pancreas/pancreas-carcinoma-1.
28. H. S. Park, J. M. Lee, H. K. Choi, S. H. Hong, J. K. Han, and B. I. Choi, "Preoperative evaluation of pancreatic cancer: Comparison of gadolinium-enhanced dynamic MRI with MR cholangiopancreatography versus MDCT," *Journal of Magnetic Resonance Imaging*, vol. 30, no. 3, pp. 586–595, Sep. 2009, doi: 10.1002/jmri.21889.
29. W. Schima and R. Függer, "Evaluation of focal pancreatic masses: comparison of mangafodipir-enhanced MR imaging and contrast-enhanced helical CT," *Eur Radiol*, vol. 12, no. 12, pp. 2998–3008, Dec. 2002, doi: 10.1007/s00330-002-1531-y.
30. H. S. Park, J. M. Lee, H. K. Choi, S. H. Hong, J. K. Han, and B. I. Choi, "Preoperative evaluation of pancreatic cancer: Comparison of gadolinium-enhanced dynamic MRI with MR cholangiopancreatography versus MDCT," *Journal of Magnetic Resonance Imaging*, vol. 30, no. 3, pp. 586–595, Sep. 2009, doi: 10.1002/jmri.21889.
31. N. Horvat, D. E. Ryan, M. D. LaGratta, P. M. Shah, and R. K. Do, "Imaging for pancreatic ductal adenocarcinoma," *Chin Clin Oncol*, vol. 6, no. 6, pp. 62–62, Dec. 2017, doi: 10.21037/cco.2017.11.03.
32. F.-M. Chen, J.-M. Ni, Z.-Y. Zhang, L. Zhang, B. Li, and C.-J. Jiang, "Presurgical Evaluation of Pancreatic Cancer: A Comprehensive Imaging Comparison of CT Versus MRI," *American Journal of Roentgenology*, vol. 206, no. 3, pp. 526–535, Mar. 2016, doi: 10.2214/AJR.15.15236.
33. S. Rickes, K. Unkrodt, H. Neye, K. W. Ocran, and W. Wermke, "Differentiation of Pancreatic Tumours by Conventional Ultrasound, Unenhanced and Echo-Enhanced Power Doppler Sonography," *Scand J Gastroenterol*, vol. 37, no. 11, pp. 1313–1320, Jan. 2002, doi: 10.1080/003655202761020605.
34. E. S. Lee, "Imaging diagnosis of pancreatic cancer: A state-of-the-art review," *World J Gastroenterol*, vol. 20, no. 24, p. 7864, 2014, doi: 10.3748/wjg.v20.i24.7864.
35. M. Dbouk *et al.*, "The Multicenter Cancer of Pancreas Screening Study: Impact on Stage and Survival," *Journal of Clinical Oncology*, vol. 40, no. 28, pp. 3257–3266, Oct. 2022, doi: 10.1200/JCO.22.00298.
36. M. Ramaekers *et al.*, "Computer-Aided Detection for Pancreatic Cancer Diagnosis: Radiological Challenges and Future Directions," *J Clin Med*, vol. 12, no. 13, p. 4209, Jun. 2023, doi: 10.3390/jcm12134209.
37. K. M. Jang, S. H. Kim, Y. K. Kim, K. D. Song, S. J. Lee, and D. Choi, "Missed pancreatic ductal adenocarcinoma: Assessment of early imaging findings on prediagnostic magnetic resonance imaging," *Eur J Radiol*, vol. 84, no. 8, pp. 1473–1479, Aug. 2015, doi: 10.1016/j.ejrad.2015.05.012.
38. K. Cao *et al.*, "Large-scale pancreatic cancer detection via non-contrast CT and deep learning," *Nat Med*, Nov. 2023, doi: 10.1038/s41591-023-02640-w.
39. P. Korfiatis *et al.*, "Automated Artificial Intelligence Model Trained on a Large Data Set Can Detect Pancreas Cancer on Diagnostic Computed Tomography Scans As Well As Visually Occult Preinvasive Cancer on Prediagnostic Computed Tomography Scans," *Gastroenterology*, vol. 165, no. 6, pp. 1533-1546.e4, Dec. 2023, doi: 10.1053/j.gastro.2023.08.034.
40. L. C. Chu *et al.*, "Application of Deep Learning to Pancreatic Cancer Detection: Lessons Learned From Our Initial Experience," *Journal of the American College of Radiology*, vol. 16, no. 9, pp. 1338–1342, Sep. 2019, doi: 10.1016/j.jacr.2019.05.034.
41. L. C. Chu *et al.*, "Utility of CT Radiomics Features in Differentiation of Pancreatic Ductal Adenocarcinoma From Normal Pancreatic Tissue," *American Journal of Roentgenology*, vol. 213, no. 2, pp. 349–357, Aug. 2019, doi: 10.2214/AJR.18.20901.
42. L. C. Chu *et al.*, "Diagnostic performance of commercially available vs. in-house radiomics software in classification of CT images from patients with pancreatic ductal adenocarcinoma vs. healthy controls," *Abdominal Radiology*, vol. 45, no. 8, pp. 2469–2475, Aug. 2020, doi: 10.1007/s00261-020-02556-w.

43. H. Ma *et al.*, "Construction of a convolutional neural network classifier developed by computed tomography images for pancreatic cancer diagnosis," *World J Gastroenterol*, vol. 26, no. 34, pp. 5156–5168, Sep. 2020, doi: 10.3748/wjg.v26.i34.5156.
44. N. Alves, M. Schuurmans, G. Litjens, J. S. Bosma, J. Hermans, and H. Huisman, "Fully Automatic Deep Learning Framework for Pancreatic Ductal Adenocarcinoma Detection on Computed Tomography," *Cancers (Basel)*, vol. 14, no. 2, p. 376, Jan. 2022, doi: 10.3390/cancers14020376.
45. S. Mukherjee *et al.*, "Radiomics-based Machine-learning Models Can Detect Pancreatic Cancer on Prediagnostic Computed Tomography Scans at a Substantial Lead Time Before Clinical Diagnosis," *Gastroenterology*, vol. 163, no. 5, pp. 1435-1446.e3, Nov. 2022, doi: 10.1053/j.gastro.2022.06.066.
46. S. Wang *et al.*, "Compute Tomography Radiomics Analysis on Whole Pancreas Between Healthy Individual and Pancreatic Ductal Adenocarcinoma Patients: Uncertainty Analysis and Predictive Modeling," *Technol Cancer Res Treat*, vol. 21, 2022, doi: 10.1177/15330338221126869.
47. P.-T. Chen *et al.*, "Radiomic Features at CT Can Distinguish Pancreatic Cancer from Noncancerous Pancreas," *Radiol Imaging Cancer*, vol. 3, no. 4, p. e210010, Jul. 2021, doi: 10.1148/rycan.2021210010.
48. L. C. Chu *et al.*, "Utility of CT Radiomics Features in Differentiation of Pancreatic Ductal Adenocarcinoma From Normal Pancreatic Tissue," *American Journal of Roentgenology*, vol. 213, no. 2, pp. 349–357, Aug. 2019, doi: 10.2214/AJR.18.20901.
49. C. G. A. Viviers *et al.*, "Improved Pancreatic Tumor Detection by Utilizing Clinically-Relevant Secondary Features," Aug. 2022, [Online]. Available: http://arxiv.org/abs/2208.03581
50. E. M. Weisberg *et al.*, "Deep lessons learned: Radiology, oncology, pathology, and computer science experts unite around artificial intelligence to strive for earlier pancreatic cancer diagnosis," *Diagn Interv Imaging*, vol. 101, no. 2, pp. 111–115, Feb. 2020, doi: 10.1016/j.diii.2019.09.002.
51. A. Farag, L. Lu, H. R. Roth, J. Liu, E. Turkbey, and R. M. Summers, "A Bottom-Up Approach for Pancreas Segmentation Using Cascaded Superpixels and (Deep) Image Patch Labeling," *IEEE Transactions on Image Processing*, vol. 26, no. 1, pp. 386–399, Jan. 2017, doi: 10.1109/TIP.2016.2624198.
52. Y. Zhou *et al.*, "Hyper-Pairing Network for Multi-phase Pancreatic Ductal Adenocarcinoma Segmentation," 2019, pp. 155–163. doi: 10.1007/978-3-030-32245-8_18.
53. Z. Zhu, Y. Xia, L. Xie, E. K. Fishman, and A. L. Yuille, "Multi-Scale Coarse-to-Fine Segmentation for Screening Pancreatic Ductal Adenocarcinoma," Jul. 2018.
54. M. Barat *et al.*, "Artificial intelligence: a critical review of current applications in pancreatic imaging," *Japanese Journal of Radiology*, vol. 39, no. 6. Springer Japan, pp. 514–523, Jun. 01, 2021. doi: 10.1007/s11604-021-01098-5.
55. L.-C. Chen, G. Papandreou, I. Kokkinos, K. Murphy, and A. L. Yuille, "DeepLab: Semantic Image Segmentation with Deep Convolutional Nets, Atrous Convolution, and Fully Connected CRFs," *IEEE Trans Pattern Anal Mach Intell*, vol. 40, no. 4, pp. 834–848, Apr. 2018, doi: 10.1109/TPAMI.2017.2699184.
56. F. Chollet, "Xception: Deep Learning with Depthwise Separable Convolutions," in *2017 IEEE Conference on Computer Vision and Pattern Recognition (CVPR)*, IEEE, Jul. 2017, pp. 1800–1807. doi: 10.1109/CVPR.2017.195.
57. H. Ni *et al.*, "Predicting Recurrence in Pancreatic Ductal Adenocarcinoma after Radical Surgery Using an AX-Unet Pancreas Segmentation Model and Dynamic Nomogram," *Bioengineering*, vol. 10, no. 7, Jul. 2023, doi: 10.3390/bioengineering10070828.
58. A. Turečková, T. Tureček, Z. Komínková Oplatková, and A. Rodríguez-Sánchez, "Improving CT Image Tumor Segmentation Through Deep Supervision and Attentional Gates," *Front Robot AI*, vol. 7, Aug. 2020, doi: 10.3389/frobt.2020.00106.
59. A. L. Simpson *et al.*, "A large annotated medical image dataset for the development and evaluation of segmentation algorithms," Feb. 2019.
60. F. Isensee *et al.*, "nnU-Net: Self-adapting Framework for U-Net-Based Medical Image Segmentation," Sep. 2018.
61. Y. Zhou *et al.*, "Hyper-Pairing Network for Multi-phase Pancreatic Ductal Adenocarcinoma Segmentation," 2019, pp. 155–163. doi: 10.1007/978-3-030-32245-8_18.
62. T. Mahmoudi *et al.*, "Segmentation of pancreatic ductal adenocarcinoma (PDAC) and surrounding vessels in CT images using deep convolutional neural networks and texture descriptors," *Sci Rep*, vol. 12, no. 1, p. 3092, Feb. 2022, doi: 10.1038/s41598-022-07111-9.
63. C. Shen *et al.*, "A cascaded fully convolutional network framework for dilated pancreatic duct segmentation," *Int J Comput Assist Radiol Surg*, vol. 17, no. 2, pp. 343–354, Feb. 2022, doi: 10.1007/s11548-021-02530-x.
64. J. Lu, N. Jiang, Y. Zhang, and D. Li, "A CT based radiomics nomogram for differentiation between focal-type autoimmune pancreatitis and pancreatic ductal adenocarcinoma," *Front Oncol*, vol. 13, Mar. 2023, doi: 10.3389/fonc.2023.979437.
65. S. Park *et al.*, "Differentiating autoimmune pancreatitis from pancreatic ductal adenocarcinoma with CT radiomics features," *Diagn Interv Imaging*, vol. 101, no. 9, pp. 555–564, Sep. 2020, doi: 10.1016/j.diii.2020.03.002.

66. K. Anai *et al.*, "The effect of CT texture-based analysis using machine learning approaches on radiologists' performance in differentiating focal-type autoimmune pancreatitis and pancreatic duct carcinoma," *Jpn J Radiol*, vol. 40, no. 11, pp. 1156–1165, Nov. 2022, doi: 10.1007/s11604-022-01298-7.
67. Y. Deng *et al.*, "Radiomics Model Based on MR Images to Discriminate Pancreatic Ductal Adenocarcinoma and Mass-Forming Chronic Pancreatitis Lesions," *Front Oncol*, vol. 11, Mar. 2021, doi: 10.3389/fonc.2021.620981.
68. S. Ren *et al.*, "Computed Tomography-Based Radiomics Signature for the Preoperative Differentiation of Pancreatic Adenosquamous Carcinoma From Pancreatic Ductal Adenocarcinoma," *Front Oncol*, vol. 10, Aug. 2020, doi: 10.3389/fonc.2020.01618.
69. Y. J. Shi *et al.*, "Histogram array and convolutional neural network of DWI for differentiating pancreatic ductal adenocarcinomas from solid pseudopapillary neoplasms and neuroendocrine neoplasms," *Clin Imaging*, vol. 96, pp. 15–22, Apr. 2023, doi: 10.1016/j.clinimag.2023.01.008.
70. G. Younan, "Pancreas Solid Tumors," *Surgical Clinics of North America*, vol. 100, no. 3, pp. 565–580, Jun. 2020, doi: 10.1016/J.SUC.2020.02.008.
71. T. Zhang *et al.*, "Radiomics Combined with Multiple Machine Learning Algorithms in Differentiating Pancreatic Ductal Adenocarcinoma from Pancreatic Neuroendocrine Tumor: More Hands Produce a Stronger Flame," *J Clin Med*, vol. 11, no. 22, Nov. 2022, doi: 10.3390/jcm11226789.
72. N. Macías *et al.*, "Histologic Tumor Grade and Preoperative Bilary Drainage are the Unique Independent Prognostic Factors of Survival in Pancreatic Ductal Adenocarcinoma Patients After Pancreaticoduodenectomy," *J Clin Gastroenterol*, vol. 52, no. 2, pp. e11–e17, Feb. 2018, doi: 10.1097/MCG.0000000000000793.
73. K. F. D. Kuhlmann *et al.*, "Surgical treatment of pancreatic adenocarcinoma," *Eur J Cancer*, vol. 40, no. 4, pp. 549–558, Mar. 2004, doi: 10.1016/j.ejca.2003.10.026.
74. S. H. Han *et al.*, "Actual long-term outcome of T1 and T2 pancreatic ductal adenocarcinoma after surgical resection," *International Journal of Surgery*, vol. 40, pp. 68–72, Apr. 2017, doi: 10.1016/j.ijsu.2017.02.007.
75. M. Schuurmans, N. Alves, P. Vendittelli, H. Huisman, and J. Hermans, "Setting the Research Agenda for Clinical Artificial Intelligence in Pancreatic Adenocarcinoma Imaging," *Cancers (Basel)*, vol. 14, no. 14, p. 3498, Jul. 2022, doi: 10.3390/cancers14143498.
76. H. Fu *et al.*, "Automatic Pancreatic Ductal Adenocarcinoma Detection in Whole Slide Images Using Deep Convolutional Neural Networks," *Front Oncol*, vol. 11, Jun. 2021, doi: 10.3389/fonc.2021.665929.
77. P. Sántha *et al.*, "Morphological Heterogeneity in Pancreatic Cancer Reflects Structural and Functional Divergence," *Cancers (Basel)*, vol. 13, no. 4, p. 895, Feb. 2021, doi: 10.3390/cancers13040895.
78. V. Baxi, R. Edwards, M. Montalto, and S. Saha, "Digital pathology and artificial intelligence in translational medicine and clinical practice," *Modern Pathology*, vol. 35, no. 1, pp. 23–32, Jan. 2022, doi: 10.1038/s41379-021-00919-2.
79. W. Qiu *et al.*, "Pancreatic ductal adenocarcinoma: Machine learning–based quantitative computed tomography texture analysis for prediction of histopathological grade," *Cancer Manag Res*, vol. 11, pp. 9253–9264, 2019, doi: 10.2147/CMAR.S218414.
80. C. Cen *et al.*, "Clinical-radiomics nomogram using contrast-enhanced CT to predict histological grade and survival in pancreatic ductal adenocarcinoma," *Front Oncol*, vol. 13, 2023, doi: 10.3389/fonc.2023.1218128.
81. A. Makohon-Moore and C. A. Iacobuzio-Donahue, "Pancreatic cancer biology and genetics from an evolutionary perspective," *Nat Rev Cancer*, vol. 16, no. 9, pp. 553–565, Sep. 2016, doi: 10.1038/nrc.2016.66.
82. R. Hinzpeter *et al.*, "CT Radiomics and Whole Genome Sequencing in Patients with Pancreatic Ductal Adenocarcinoma: Predictive Radiogenomics Modeling," *Cancers (Basel)*, vol. 14, no. 24, Dec. 2022, doi: 10.3390/cancers14246224.
83. J. Gao *et al.*, "Differentiating TP53 Mutation Status in Pancreatic Ductal Adenocarcinoma Using Multiparametric MRI-Derived Radiomics," *Front Oncol*, vol. 11, May 2021, doi: 10.3389/fonc.2021.632130.
84. P. Chaturvedi *et al.*, "MUC4 Mucin Potentiates Pancreatic Tumor Cell Proliferation, Survival, and Invasive Properties and Interferes with Its Interaction to Extracellular Matrix Proteins," *Molecular Cancer Research*, vol. 5, no. 4, pp. 309–320, Apr. 2007, doi: 10.1158/1541-7786.MCR-06-0353.
85. M. Mimeault, S. L. Johansson, S. Senapati, N. Momi, S. Chakraborty, and S. K. Batra, "MUC4 down-regulation reverses chemoresistance of pancreatic cancer stem/progenitor cells and their progenies," *Cancer Lett*, vol. 295, no. 1, pp. 69–84, Sep. 2010, doi: 10.1016/j.canlet.2010.02.015.
86. M. Saitou, "MUC4 expression is a novel prognostic factor in patients with invasive ductal carcinoma of the pancreas," *J Clin Pathol*, vol. 58, no. 8, pp. 845–852, Aug. 2005, doi: 10.1136/jcp.2004.023572.
87. Y. Deng *et al.*, "Radiomics models based on multi-sequence MRI for preoperative evaluation of MUC4 status in pancreatic ductal adenocarcinoma: a preliminary study," *Quant Imaging Med Surg*, vol. 12, no. 11, pp. 5129–5139, Nov. 2022, doi: 10.21037/qims-22-112.
88. Y. Iwatate *et al.*, "Radiogenomics for predicting p53 status, PD-L1 expression, and prognosis with machine learning in pancreatic cancer," *Br J Cancer*, vol. 123, no. 8, pp. 1253–1261, Oct. 2020, doi: 10.1038/s41416-020-0997-1.

89. Y. Meng *et al.*, "Noncontrast Magnetic Resonance Radiomics and Multilayer Perceptron Network Classifier: An approach for Predicting Fibroblast Activation Protein Expression in Patients With Pancreatic Ductal Adenocarcinoma," *Journal of Magnetic Resonance Imaging*, vol. 54, no. 5, pp. 1432–1443, Nov. 2021, doi: 10.1002/jmri.27648.
90. I. Vezakis *et al.*, "An Automated Prognostic Model for Pancreatic Ductal Adenocarcinoma," *Genes (Basel)*, vol. 14, no. 9, Sep. 2023, doi: 10.3390/genes14091742.
91. X. Xu, J. Qu, Y. Zhang, X. Qian, T. Chen, and Y. Liu, "Development and validation of an MRI-radiomics nomogram for the prognosis of pancreatic ductal adenocarcinoma," *Front Oncol*, vol. 13, 2023, doi: 10.3389/fonc.2023.1074445.
92. H. Qiu *et al.*, "Original Article A novel preoperative MRI-based radiomics nomogram outperforms traditional models for prognostic prediction in pancreatic ductal adenocarcinoma," 2022. [Online]. Available: www.ajcr.us/
93. X. Li *et al.*, "Preoperative recurrence prediction in pancreatic ductal adenocarcinoma after radical resection using radiomics of diagnostic computed tomography," *EClinicalMedicine*, vol. 43, Jan. 2022, doi: 10.1016/j.eclinm.2021.101215.
94. T. Xie, X. Wang, M. Li, T. Tong, X. Yu, and Z. Zhou, "Pancreatic ductal adenocarcinoma: a radiomics nomogram outperforms clinical model and TNM staging for survival estimation after curative resection," *Eur Radiol*, vol. 30, no. 5, pp. 2513–2524, May 2020, doi: 10.1007/s00330-019-06600-2.
95. S. Park *et al.*, "CT Radiomics–Based Preoperative Survival Prediction in Patients With Pancreatic Ductal Adenocarcinoma," *American Journal of Roentgenology*, vol. 217, no. 5, pp. 1104–1112, Nov. 2021, doi: 10.2214/AJR.20.23490.
96. F. Chen *et al.*, "Radiomics-Assisted Presurgical Prediction for Surgical Portal Vein-Superior Mesenteric Vein Invasion in Pancreatic Ductal Adenocarcinoma," *Front Oncol*, vol. 10, Nov. 2020, doi: 10.3389/fonc.2020.523543.
97. J. K. Jang *et al.*, "CT-determined resectability of borderline resectable and unresectable pancreatic adenocarcinoma following FOLFIRINOX therapy," *Eur Radiol*, vol. 31, no. 2, pp. 813–823, Feb. 2021, doi: 10.1007/s00330-020-07188-8.
98. M. Zins, C. Matos, and C. Cassinotto, "Pancreatic Adenocarcinoma Staging in the Era of Preoperative Chemotherapy and Radiation Therapy," *Radiology*, vol. 287, no. 2, pp. 374–390, May 2018, doi: 10.1148/radiol.2018171670.
99. L. Shi, L. Wang, C. Wu, Y. Wei, Y. Zhang, and J. Chen, "Preoperative Prediction of Lymph Node Metastasis of Pancreatic Ductal Adenocarcinoma Based on a Radiomics Nomogram of Dual-Parametric MRI Imaging," *Front Oncol*, vol. 12, Jul. 2022, doi: 10.3389/fonc.2022.927077.
100. Y. Bian *et al.*, "Radiomics nomogram for the preoperative prediction of lymph node metastasis in pancreatic ductal adenocarcinoma," *Cancer Imaging*, vol. 22, no. 1, Dec. 2022, doi: 10.1186/s40644-021-00443-1.
101. J. Chang *et al.*, "Machine-learning based investigation of prognostic indicators for oncological outcome of pancreatic ductal adenocarcinoma," *Front Oncol*, vol. 12, Dec. 2022, doi: 10.3389/fonc.2022.895515.